Selection of Top Layer Materials for Gas–Liquid Membrane Contactors

D. C. Nymeijer, B. Folkers, I. Breebaart, M. H. V. Mulder, M. Wessling

Membrane Technology Group, Department of Science and Technology, University of Twente, P.O. Box 217, 7500 AE Enschede, The Netherlands

Received 18 June 2003; accepted 10 October 2003

ABSTRACT: Gas–liquid membrane contactors frequently suffer from wetting of the microporous membrane. Stabilization layers at the liquid side of the membrane potentially prevent this wetting. We applied such stabilized membranes to the separation of olefins and paraffins using $AgNO_3$ solutions as absorption liquid. The stabilization material requires permeation of olefins at minimum counter transport of water. Appropriate selection of the top layer material is crucial in this application. This report describes the selection of potential top layer materials. Dense films of the selected materials were prepared and used to determine ethylene and ethane permeabilities, to perform pervaporation experiments with water and a 3.5*M* solution of silver nitrate in water, and to determine the swelling behavior of the dense films in water and in a 3.5*M* silver nitrate solution. Based on the characterization experiments, ethylene propylenediene terpolymer is the most appropriate candidate with the highest potential for application in a gas–liquid membrane contactor for the separation of paraffins and olefins. It has a relatively high olefin permeability (46.4 Barrer) and a corresponding low water vapor permeability and low swelling tendency in a 3.5*M* silver nitrate solution (1490 Barrer and 0.14 wt %, respectively). © 2004 Wiley Periodicals, Inc. J Appl Polym Sci 92: 323–334, 2004

Key words: membranes; olefin/paraffin separation; elastomers; films; pervaporation

INTRODUCTION

Gas–liquid membrane contactors offer a unique way to perform gas–liquid absorption processes in a controlled fashion: membrane contactors have a large operation flexibility and the gas and the liquid flow can be controlled independently as opposed to state-of-the-art packed column devices.[1]

In a gas–liquid membrane contactor, separation of a gas mixture is achieved by the absorption liquid, which selectively absorbs one of the components of the permeating gas mixture, whereas the membrane, which is generally microporous, acts as a nonselective barrier between the gas and the liquid phase. A specific application of a gas–liquid membrane contacting system is the selective absorption of olefins from a feed mixture of paraffins and olefins using a concentrated silver nitrate solution. Separation of paraffins and olefins is one of the most important processes in the petrochemical industry.[2] Conventional separations like distillation are difficult and expensive because of the physical similarity of paraffins and olefins. In a gas–liquid membrane contactor, the separation is based on the ability of silver ions to form a complex with the double bond of the olefin.[3] The main problem of gas–liquid membrane contactors is wetting or flooding of the microporous membrane and thus increasing the resistance to mass transport. To avoid this, the application of composite membranes consisting of a porous support and a dense coating layer on top of this support is required. Bessarabov et al.[4] described the application of a composite membrane having a PDMS-like top layer; however, the motivation for material selection for membrane preparation remains open in their article.

The present work describes a systematic selection of potential coating layer materials. Gas permeation experiments were performed and related to vapor permeation and swelling behavior of a variety of elastomers. Based on the experiments, the ratio of the ethylene permeability and the water vapor permeability was determined and used as the criterion to select suitable coating materials for application in a gas–liquid membrane contactor for olefin/paraffin separation.

THEORETICAL BACKGROUND

In gas–liquid membrane contactors, a gas phase and a liquid phase are brought into contact by means of a membrane. This allows controlled mass transport of one of the components of the feed gas mixture into the absorption liquid. The total flux of a component from

Correspondence to: M. Wessling (m.wessling@utwente.nl).
Contract grant sponsor: Centre for Separation Technology.

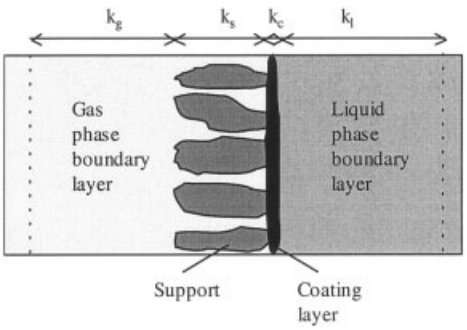

Figure 1 Schematic presentation of the resistances of a gas–liquid membrane contactor with a composite membrane as interface between gas and liquid phase.

the gas phase, through the porous support and the dense top layer into the liquid phase, is expressed as

$$J = K_{ov}\Delta c \tag{1}$$

where J is the total ethylene flux of the component, Δc is the driving force for transport of the component, and K_{ov} is the overall mass transfer coefficient. The overall resistance to mass transfer ($1/K_{ov}$) depends, in the case composite membranes are used, on four consecutive resistances in series (Fig. 1): the resistance of the gas phase boundary layer ($1/k_g$), the resistance of the porous support ($1/k_s$), the resistance of the dense coating layer ($1/k_c$), and the resistance of the liquid phase boundary layer ($1/k_l$).

In the case of olefin/paraffin separation, a silver salt solution was used as absorption liquid and after permeation through the membrane, complex formation between the positively charged silver ions and the double bond of ethylene occurred. In contrast, ethane was only physically absorbed. With respect to chemisorption, the overall resistance to olefin transport can be written as

$$\frac{1}{K_{ov}} = \frac{1}{k_g} + \frac{1}{k_s} + \frac{1}{k_c} + \frac{1}{mE_a k_l} \tag{2}$$

Typical values for the individual mass transfer coefficients are given in Table I. Table I indicates that the resistance of the gas phase and the membrane support are relatively small compared to the corresponding values of the top layer and the liquid phase. Depending on the process conditions and the corresponding resistance of the liquid phase, mass transfer of olefins through the dense top layer can become the limiting step in the separation process. However, this is undesirable because the selectivity of the process decreases as well as a result of the low intrinsic selectivity of the coating layer material.[4]

Transport of olefins through the dense coating layer is quantified by the permeability (P_i) of the olefin through the layer, which in turn is a function of the solubility (S_i) and the diffusivity (D_i) of the olefin in the layer:

$$P_i = D_i S_i \tag{3}$$

The requirements for the membranes used in olefin/paraffin membrane contactor applications are (1) high permeability for hydrocarbons, (2) stability in a hydrocarbon environment, (3) low permeability for vapors of the absorption liquid, (4) stability in the selective liquid absorbent, (5) good mechanical properties, and (6) resistance to pore flooding by the absorption liquid.[4] To fulfill these requirements, composite membranes with dense polymeric top layers on top of a microporous support are required. The support membrane is of minor importance, but the top layer material is crucial in this application.

With this work we aimed to identify potential materials that fulfill these requirements. The selection of potential materials to be investigated was based on three criteria:

1. The material should be highly permeable for ethylene. We therefore restricted the selection to the group of elastomers.
2. The material should be hydrophobic.[11] The absorption liquid used is an aqueous solution and the top layer material should prevent permeation of this liquid into the gas phase.
3. The material should be commercially available. Olefins and paraffins are bulk chemicals produced in large amounts and the separation of both components is one of the most important processes in the petrochemical industry. To make gas–liquid membrane contactors an attractive replacement for conventional separation methods (e.g., distillation), the existence of cheap membranes is necessary, requiring the commercial availability of the materials.

For screening, gas permeation, pervaporation, and swelling experiments were performed with dense films of the selected elastomers. In gas permeation experiments, nitrogen, carbon dioxide, ethylene, and

TABLE I
Typical Values for Mass Transfer Coefficients (k_i) and Corresponding Resistances to Mass Transfer ($1/k_i$)[a]

Phase	Mass transfer coefficient	Typical value (k_i) (m/s)	Typical value ($1/k_t$) (s/m)
Gas	k_g	10^{-2}–10^{-1}	10^{1}–10^{2}
Support	k_s	10^{-3}–10^{-2}	10^{2}–10^{3}
Coating	k_c	10^{-5}–10^{-4}	10^{4}–10^{5}
Liquid	k_l	10^{-5}–10^{-4}	10^{4}–10^{5}

[a] Refs. 5–10.

ethane permeabilities were determined and the activation energies for permeation were calculated, the latter being important for the overall process, given that absorption and desorption normally operate at different temperatures.

Pervaporation experiments with water and a 3.5*M* solution of silver nitrate in water were performed to determine the possible amount of counterpermeation of water through the dense top layer. Finally, swelling of the dense films in water and in a 3.5*M* silver nitrate solution was determined to investigate the material properties in the swollen state.

EXPERIMENTAL

Materials

The polymers used are listed in Table II. They were kindly supplied by Helvoet BV, Hellevoetsluis, The Netherlands. The molecular structure, the composition, the glass-transition temperature, and the amount of free volume of the polymers are also mentioned. Glass-transition temperatures were taken from the literature[12,13] and the amount of free volume was calculated using the group contribution theory of van Krevelen.[14,15] The last column gives the average thickness l_{av} of the prepared polymer films as determined using a screw micrometer and averaging the thickness measured at different locations. The elastomers mentioned in Table II were chosen based on their hydrophobicity, commercial availability, and processability. Therefore, the type of PEBAX® used has a hydrophobic character. To investigate the influence of acrylonitrile part in NBR, we systematically varied the amount of acrylonitrile in the polymer.

The solvent used to dissolve the polymers is either *n*-hexane (EPDM), formic acid (PEBAX), or chloroform (other elastomers). The chemicals were purchased from Merck (The Netherlands) and used without further purification. The crosslink initiator was dicumyl peroxide (DCP), purchased from Aldrich (The Netherlands). Nitrogen (99.9%), carbon dioxide (99.95%), methane (99.95%), ethane (99.5%), ethylene (99.9%), propane (99.95%), and propylene (99.8%) for gas permeation experiments were supplied by Hoekloos (The Netherlands). For the swelling and pervaporation experiments ultrapure water (resistivity $> 18.0 M\Omega\ cm^{-1}$ at 25°C) was used. Silver nitrate from Merck was used without further purification.

Membrane preparation

The elastomers were dissolved in *n*-hexane (EPDM), formic acid (PEBAX), or chloroform (others). Solutions of 10 wt % of polymer were prepared. DCP (5 g) per 100 g polymer was added as crosslinking agent (except for PDMS and PEBAX). After dissolution of the elastomer, the solutions were filtered using a 40-μm metal filter. Films were cast onto a Teflon plate using a 1-mm casting knife. These films were placed in a nitrogen box to allow the solvent to evaporate overnight in a nitrogen atmosphere. Finally, the membranes were placed in a nitrogen oven at 150°C for 1 h to initiate crosslinking. The amount of DCP and the crosslinking temperature and time were chosen because under these conditions the swelling of the films in moderately swelling agents is independent of this amount, temperature, or time.[16] The ultimate thickness of the prepared films was determined using a digital screw micrometer (Mitutoya). The mean thickness of the prepared films is given in Table II.

Gas permeation

Gas permeation experiments were performed with the setup previously described by Bos et al.[17] After determination of the film thickness, the polymer films were put into a flat, thermostated cell in the gas permeation setup. At the permeate side of the cell, vacuum (<0.05 mbar) was applied using a high-vacuum pump (Edwards). An absolute pressure of 1 bar was applied at the feed side. The temperature of the thermostated cell was adjusted to the desired value. The effective membrane area was 11.95 cm^2. Measuring of the permeance occurred by closing the valve to the vacuum pump and measuring the increase in pressure in a calibrated volume as a function of time. With the ideal gas law and the thickness of the used films, the permeability of the material for the corresponding gases can be calculated from the pressure increase on the permeate side.

Nitrogen, carbon dioxide, ethane, and ethylene permeabilities were determined at room temperature (25°C). Because PDMS, EPDM, SBR, and CR seem to be the most promising materials for application in a gas–liquid membrane contactor, these materials were used for further experiments at elevated temperatures. These measurements were performed at 25, 30, 40, and 50°C using N_2, CO_2, CH_4, C_2H_6, C_2H_4, C_3H_8, and C_3H_6.

Pervaporation

Pervaporation experiments were performed using the setup described by Meuleman et al.[18] After determination of the thickness, the prepared dense films were placed in a flat cell. Pure water or a 3.5*M* silver nitrate solution was used as the feed solution. At the permeate side an Edwards two-stage high-vacuum pump created a vacuum of less than 1 mbar, which was measured with an Edwards absolute pressure pirani (PRM 10) and pressure indicator (Controller 1101). The permeate was collected and condensed in a cold liquid nitrogen trap. After determination of the yield

TABLE II
Elastomers Used for Screening Experiments

Elastomer	Molecular structure	Wt. %	T_g (K)	V_f (cm^3/g)	Thickness (μm)
PDMS Polydimethylsil-oxane (RTV 615)	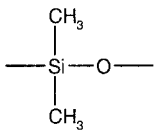	100.0	150	0.1922	200–250
EPDM Ethylene propylene terpolymer (Keltan 578)	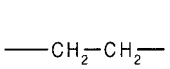	65.0 27.8	236	0.2182	45–70
	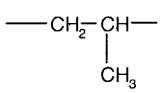				
	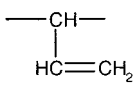	7.2			
CR Polychloroprene (Neoprene TRT)	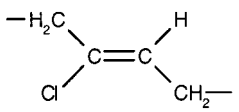	100.0	227	0.1484	90–100
HNBR Hydrogen nitrile butadiene rubber (Therban 3406)	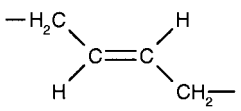	0.9	237	0.2226	110–120
	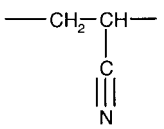	34.0			
	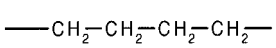	65.1			
SBR Styrene butadiene rubber (Cariflex 51502)	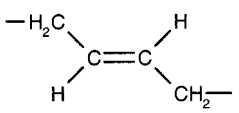	67.0	221	0.2336	90–110
	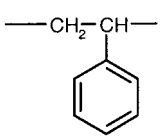	33.0			
BR 0 Butadiene rubber (Calprene 248)	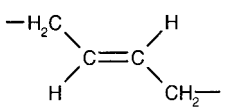	100.0	182	0.2242	80–120

TABLE II *Continued*

Elastomer	Molecular structure	Weight percentage	T_g (K)	V_f (cm^3/g)	Thickness (μm)
NBR 18 Nitrile butadiene rubber (Perbunan 1845)	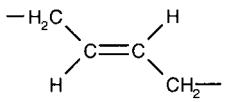	82.0	213	0.1977	80–120
	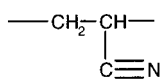	18.0			
NBR 28 Nitrile butadiene rubber (Perbunan 2846)	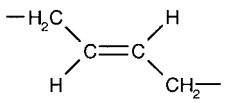	72.0	231	0.1871	80–120
	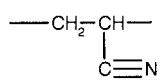	28.0			
NBR 33 Nitrile butadiene rubber (Perbunan 3446)	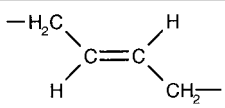	67.0	238	0.1822	80–120
	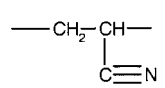	33.0			
NBR 38 Nitrile butadiene rubber (Perbunan 3945)	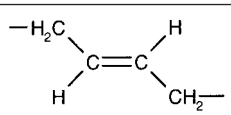	62.0	255	0.1776	80–120
	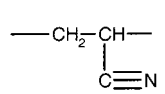	38.0			
CSPE Chlorosulfonated polyethylene (Hypalon 40)	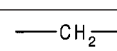	51.0	251	0.0698	90–120
	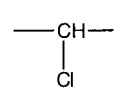	45.6			
	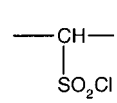	3.4			
PEBAX® Poly(amide-6-*b*-ethylene oxide) (PEBAX® 3533)	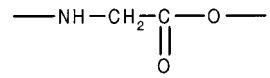	27.1	160	0.1527	80–120
	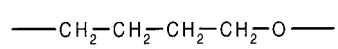	72.9			

by weighing, the permeation was calculated using the following equation:

$$P = \frac{JV_m l}{MA\Delta p} \quad (4)$$

where P is the permeability as calculated from the number of moles water collected [cm^3 (STP) $\times$ cm/s^{-1} $\times$ cm^{-2} $\times$ cmHg], J is the flux through the membrane, V_m is the molar gas volume at STP, l is the thickness of the film, M is the molecular weight of water, A is the membrane surface area, and Δp is the partial pressure difference across the membrane. The partial pressure in fact equals the equilibrium vapor pressure because the permeate pressure equals zero. In the case of pervaporation using a silver nitrate solution, the equilibrium vapor pressure was lower because of the high concentration of silver nitrate in the feed. The exact method of estimating Δp for the experiments involving the salt solution is described later.

In the case of PDMS and EPDM, two of the most promising materials, the permeate was analyzed using atomic absorption spectroscopy (AAS; Spectra 10, Varian, The Netherlands) to determine the silver ion concentration in the permeate.

Swelling

Pieces (4 $\times$ 4 cm) were cut from the polymer films. The mass of each piece was determined and the pieces were placed in petri dishes filled with either ultrapure water or a 3.5*M* $AgNO_3$ solution. After 8 h of swelling at room temperature, the pieces were removed from the petri dish and carefully dried between two tissue papers, after which the mass of the swollen film was determined subsequently. The weight increase attributed to swelling of the films (*SD*) is expressed as

$$SD = \frac{w_{\text{swollen}} - w_{\text{dry}}}{w_{\text{dry}}} \times 100\% \quad (5)$$

where w_{swollen} is the weight of the swollen film and w_{dry} is the weight of the dry film.

X-ray fluorescence

After pervaporation or swelling experiments, films of two of the most promising materials for gas–liquid membrane contactor applications, PDMS and EPDM, were dried in a vacuum oven at 30°C for at least 72 h to evaporate the water. The amount of silver ions in the dry PDMS and EPDM films was determined by X-ray fluorescence (XRF). XRF allows determination of the exact amount of silver present per unit of membrane area by irradiating the sample with high-energy primary X-ray photons. The apparatus was calibrated using a single-point calibration method and the data of the sample were corrected for the influence of the polymer matrix material. The apparatus used was a Philips PW 1480 X-ray spectrometer and the data were analyzed using a fundamental parameter method.[19]

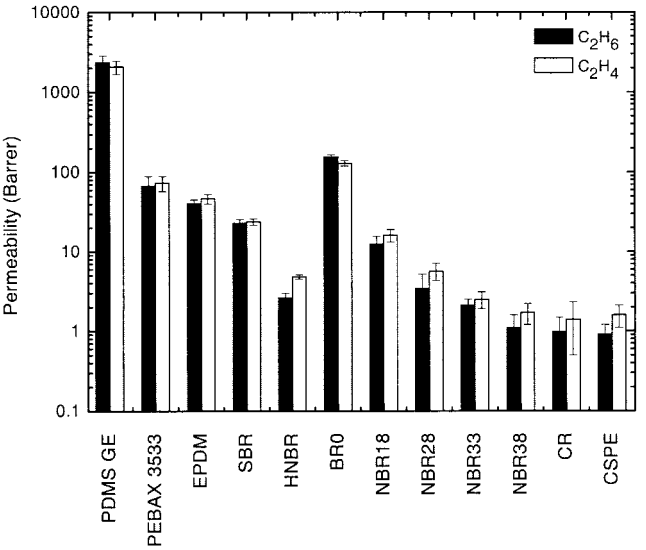

Figure 2 Ethane and ethylene permeability for different elastomers. Measurements performed at T = 25°C.

RESULTS AND DISCUSSION

Gas permeation

The results of the ethane and ethylene permeation experiments for the polymers investigated are given in Figure 2. The permeability of ethane and ethylene strongly depends on the polymer investigated and varies over $\pm$3.5 orders of magnitude.

The high permeabilities for poly(dimethylsiloxane) (PDMS) are the result of the flexible –Si—O– bond in PDMS, expressed in a low glass-transition temperature of PDMS (T_g = −123°C) and a high amount of free volume.[11,20] This results in high gas diffusion rates and corresponding high gas permeabilities.

Poly(amide-6-*b*-ethylene oxide) (PEBAX) is a block copolymer that consists of a hard crystalline polyamide segment (PA) and a soft, amorphous polyether segment (PE). The crystalline PA part acts as an impermeable phase, whereas the PE part has a relatively high permeability because of its high chain mobility. PEBAX 3533 has a PE content of 70 wt % and a crystallinity in the polymer of 6 vol %,[21] which results in relatively high gas permeabilities for PEBAX compared to that of the other elastomers investigated.

Although ethylene propylenediene terpolymer (EPDM) has a higher amount of free volume than that of PDMS and PEBAX (Table II) it has a lower gas permeability than that of either PDMS or PEBAX be-

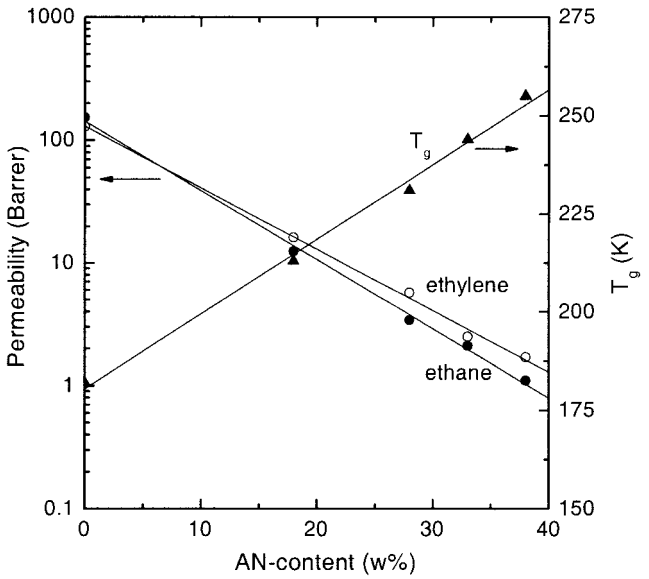

Figure 3 Permeability and glass-transition temperature of acrylonitrile rubber as a function of the acrylonitrile content. Measurements performed at T = 25°C.

cause of the considerably lower chain mobility and flexibility of EPDM,[20] visible in the higher glass-transition temperature of EPDM compared to that of PDMS and PEBAX ($T_{g,\mathrm{EPDM}}$ = −37°C, $T_{g,\mathrm{PDMS}}$ = −123°C, and $T_{g,\mathrm{PEBAX}}$ = −113°C).

The gas permeation behavior of a homologous series of butyl rubbers (NBR) containing different amounts of acrylonitrile (AN) was also investigated. The determined permeabilities and glass-transition temperatures (taken from Nijhuis et al.[11]) of this series of butyl rubber derivates as a function of the acrylonitrile (AN) contents are shown in Figure 3. Figure 4 depicts the relationship between the nitrogen permeability through the dense films and the fraction of free volume in the polymers for the homologous series of NBR elastomers. The fraction of free volume was calculated using the group contribution theory of van Krevelen.[14,15]

Figure 3 shows a strong decrease of the gas permeability and a strong increase of the glass-transition temperature with increasing AN content, a phenomenon also shown by van Amerongen[22] and Blackley.[23] The cohesive forces of the rubber molecules per unit length of the molecule determine the energy of activation for diffusion. A higher energy is required if a larger number of polar groups is present in the polymer molecules, resulting in lower diffusivities and permeabilities and higher glass-transition temperatures at higher AN content.[24] This is also visible in Figure 4. With increasing AN content (increasing amount of polar groups), the fraction of free volume linearly decreases because of the increased cohesive forces per unit length of polymer (1/FFV increases). Because diffusion of small penetrant molecules in polymers is the result of hopping of penetrant molecules from free volume pocket to free volume pocket in the polymer matrix, the nitrogen permeability decreases linearly with decreasing fraction of free volume, thus increasing the AN content.

In the case of hydrogen nitrile butadiene rubber (HNBR), which has the same AN content as that of NBR 33, the BR part of the polymer is partly replaced by its saturated variant. When the effect of the saturated C—C bond is compared to its unsaturated variant, two opposing effects influence the chain mobility of the polymer. On the one hand, C═C double bonds have a restricted rotational degree of freedom and on the other hand, it generates larger space and an increased mobility for neighboring C—C bonds.[16,20] The net result, however, is a somewhat increased chain mobility for C═C bonds compared to the saturated C—C bond. However, this is not visible in the gas permeation results because the effect of decreased chain mobility attributed to saturation is small.[16]

In SBR the AN groups of NBR 33 are replaced by an aromatic styrene group. Bulky side groups, like styrene, give rise to increased chain stiffness attributed to steric hindrance.[19,25] This is also visible in an increase in glass-transition temperature (−52°C) and a decrease in gas permeability (P_{C2H4} = 18.9 Barrer) compared to those of BR (T_g = −91°C, P_{C2H4} = 129.9 Barrer).

In polychloroprene (CR), one hydrogen atom of butyl rubber is replaced by a Cl atom. This results in stronger polymer chain interactions attributed to dipole forces, inducing an increase in glass-transition

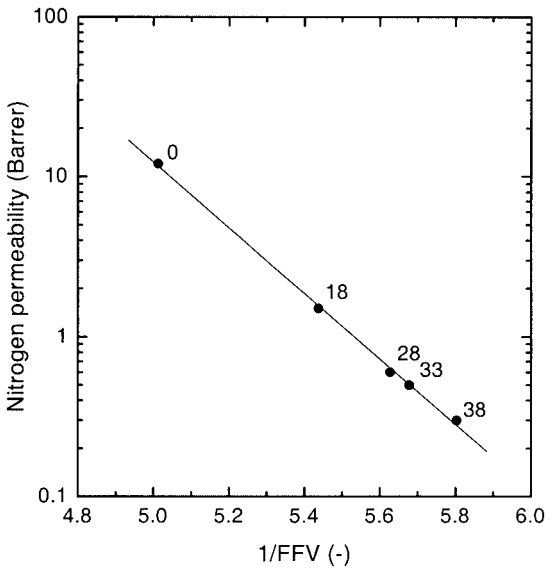

Figure 4 Nitrogen permeability of acrylonitrile rubber as a function of the fraction of free volume in the polymers. Measurements performed at T = 25°C.

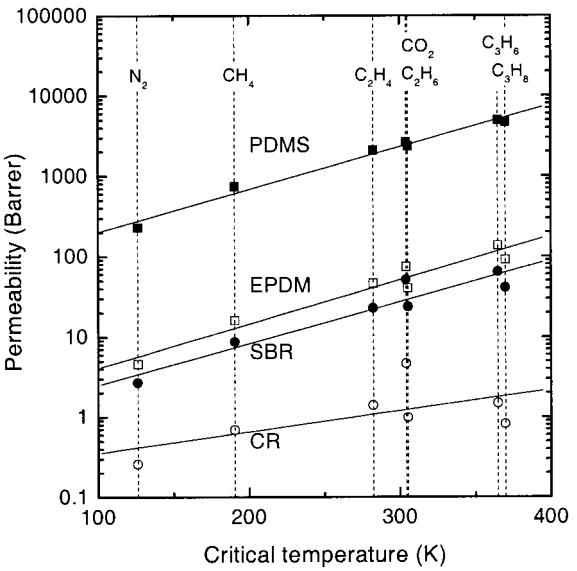

Figure 5 Permeability of several gases at 25°C for four elastomers as a function of the corresponding critical temperature of the gas.

temperature (−46°C) and a decrease in gas permeability (P_{C2H4} = 1.4 Barrer).

These dipole forces are also responsible for the relatively low gas permeabilities of chlorosulfonated polyethylene (CSPE), which contains polar Cl atoms and SO_2Cl groups.

Gas permeation at elevated temperatures

Based on the screening experiments using ethane and ethylene, a selection of four potential top layer materials was used to investigate the influence of the temperature on the gas permeation behavior of the films at 25, 30, 40, and 50°C. The result for 25°C is given in Figure 5 for different gases for PDMS, EPDM, SBR, and CR. The permeabilities are plotted as a function of the corresponding critical temperatures of the gases.[26] Because the critical temperature of a penetrant is a measure of the condensability of the penetrant molecules, this gives an indication of the solubility of penetrant molecules into the elastomeric polymer matrix. With increasing permeant size, the critical temperature of the permeant increases, resulting in higher solubilities. Increased permeant size, however, results at the same time in lower permeant diffusivities. These two opposing effects give a net increase in permeability with increasing penetrant size (see Fig. 5), indicating that the solubility plays a major role and strongly influences the permeability of the elastomers.[27] The permeabilities of the penetrants decrease in the order $C_3H_8 \approx C_3H_6 > C_2H_6 \approx CO_2 > C_2H_4 > CH_4 > N_2$. This is in accordance with the results found by Stern et al.[25] and Merkel et al.[28] We hypothesize that the relatively high permeability of the polar CO_2 and the relatively low permeabilities of the other, hydrocarbon permeants in CR compared to that of the other polymers stem from differences in solubility of the permeating species in polar (CR) or hydrocarbon-like (PDMS, EPDM, SBR) polymer matrices, as will be explained later.

Because transport through dense films can be considered as an activated process, temperature strongly influences the permeability according to an Arrhenius type of equation:

$$P = P_0 e^{(-E_p/RT)} \tag{6}$$

where P_0 is the preexponential permeability factor, T is the absolute temperature, and E_p is the activation energy for permeation. Because the gas permeability is related to the solubility and the diffusivity of a permeant in a polymer, the activation energy for permeation is a function of the heat of solution (ΔH_s) and of the activation energy for diffusion (E_d).

Together with the permeability results at different temperatures, eq. (6) can be used to calculate the activation energy for permeation. The results for PDMS, EPDM, SBR, and CR as a function of the permeant critical temperature are given in Figure 6.

Besides the permeant critical temperature, polymer–penetrant interactions relative to polymer–polymer interactions also influence the sorption of permeants in polymers.[28,29] Figure 6 visualizes this effect. The activation energy for permeation for CR increases with increasing permeant size, indicating less-favorable interactions between higher hydrocarbons and the poly-

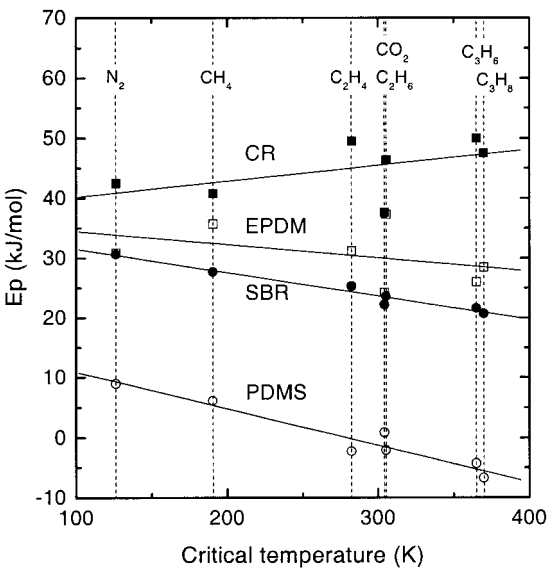

Figure 6 Activation energy for permeation of several gases for four elastomers as a function of the corresponding critical temperature of the permeating gas.

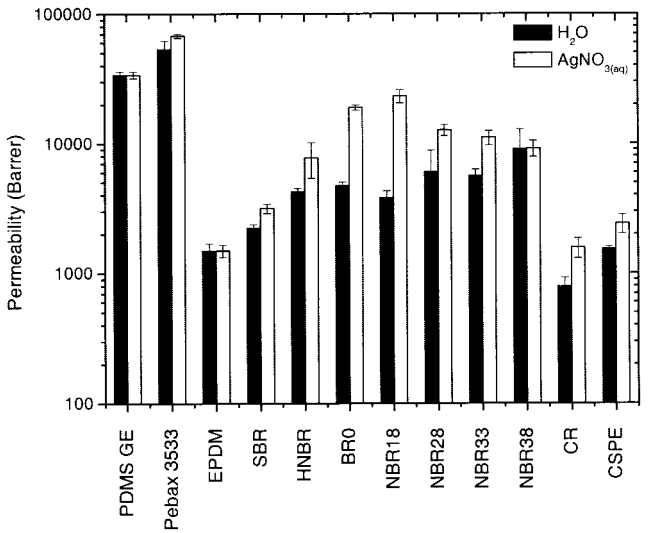

Figure 7 Pervaporation behavior of elastomers. Feed solution water (black columns) or 3.5*M* $AgNO_{3(aq)}$ (white columns). Measurements performed at $T = 25°C$.

mer matrix. The activation energy for permeation for PDMS, EPDM, and SBR decreases with increasing permeant size, indicating more favorable interactions between polymer and permeant with increasing hydrocarbon length. This explains the relatively low permeability of CR for the penetrants investigated. CR contains polar chlorine atoms, whereas the other three elastomers have a nonpolar, hydrocarbon-like structure. The solubility of the hydrocarbons in the polar, less hydrocarbon-like CR is lower than that of their corresponding values in hydrocarbon matrices like EPDM, PDMS, and SBR. The larger the hydrocarbon molecule, the more pronounced the effect. The relatively high permeability for CO_2 in CR compared to that of the other penetrants is also caused by a specific interaction between CO_2 and the polar chlorine containing polymer matrix.

Pervaporation and swelling

The results of the pervaporation experiments with water or a 3.5*M* solution of $AgNO_3$ are shown in Figure 7. The water permeability was calculated using eq. (4). The driving force for pervaporation with a silver nitrate solution as feed was calculated from the assumption that polymers that are assumed to have no particular chemical affinity with Ag^+ (PDMS, EPDM) should have the same water permeability if pure water or a solution of silver nitrate in water is used as feed. This should result in equal permeability values for water as a pure feed or in the presence of silver nitrate for PDMS and EPDM. The effective driving force for water permeation using a 3.5*M* silver nitrate solution as feed was estimated to be 1.41 cmHg compared to a value of 1.96 cmHg for ultrapure water.

Figure 8 shows the weight increase of the films attributed to water uptake when exposed for 8 h to water or to a 3.5*M* silver nitrate solution. If the permeability and the swelling results in pure water and a solution of silver nitrate are compared it becomes clear that there a one-to-one correlation does not exist between the permeability and the weight increase atributed to swelling for most elastomers. The values obtained strongly depend on the polymer investigated. The permeability varies over 1.5 orders of magnitude (Fig. 7), whereas the swelling varies over 3 orders of magnitude (Fig. 8). Generally speaking, the permeability and the swelling in a silver nitrate solution are higher than the corresponding values for water. The higher weight increase can be explained if the molecular weight of silver nitrate (170 g/mol) compared to that of water (18 g/mol) is taken into account. On the other hand, the chemical structure of the polymers investigated also plays an important role in the weight increase because of exposure to a salt solution. Polymers having C═C bonds in their structure especially show a considerable higher weight increase when exposed to silver nitrate solutions, compared to the weight increase when exposed to ultrapure water. We hypothesize that silver ions from the silver nitrate solution can form a complex with this double bond.[3,30,31] This effect is visible in the relatively high water permeabilities and degrees of swelling if a silver nitrate solution is used as feed for SBR, HNBR, NBR 18, 28, 33, 38, and CR. The degree of swelling in a silver nitrate solution of BR 0 could not be measured because of experimental problems in handling this completely swollen and soft, sticky film.

A confirmation that complexation between silver ions and the C═C double bond of the polymer occurs,

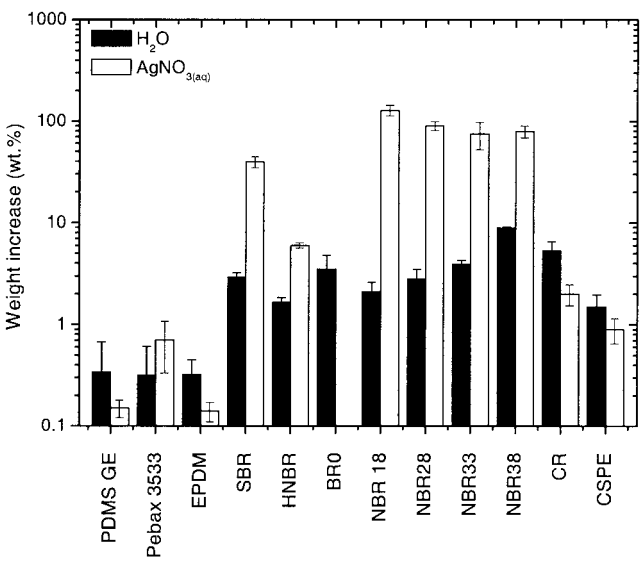

Figure 8 Swelling behavior of elastomers. Feed solution water (black columns) or 3.5*M* $AgNO_{3(aq)}$ (white columns). Measurements performed at $T = 25°C$.

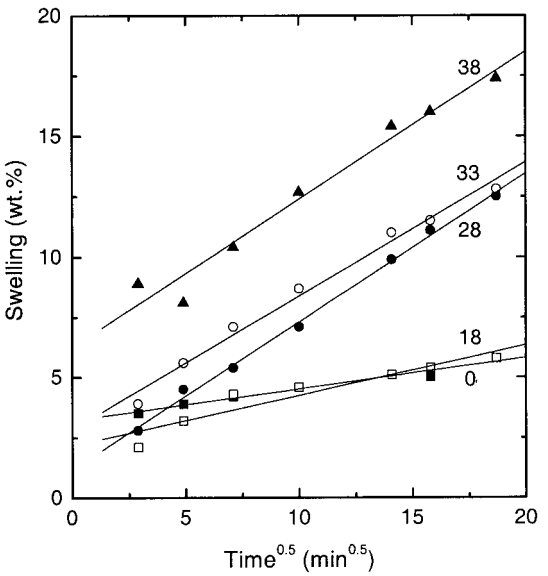

Figure 9 Swelling behavior of BR 0, NBR 18, NBR 28, NBR 33, and NBR 38 in water as a function of time. Measurements performed at $T = 25°C$.

is the pervaporation and swelling behavior of the homologous series of NBR. With increasing amount of the nitrile part (going from BR 0 to NBR 38) the permeability of water and the swelling in water increases, attributed to the more hydrophilic character of the nitrile part. The behavior in a silver nitrate solution, however, is opposite: with increasing nitrile content, the relative amount of C═C double bonds decreases and the permeation of water using a silver nitrate solution and the swelling in a silver nitrate solution also decreases. Furthermore, 72 h after the pervaporation or swelling experiments with a silver nitrate solution and exposure to daylight, the films of these materials were completely black, caused by the reduction of the positively charged silver ions under the influence of light. The films of the other materials did not change their color after contact with a silver nitrate solution. One may think that this large extent of silver absorption may have technical benefits because it would allow an ethylene-selective complexation already in the coating layer material. Unfortunately, and in contrast to the other materials, the swelling of BR 0, NBR 18, 28, 33, and 38 continuously increases in time. Even though the materials are crosslinked, they still change in time and lose their mechanical integrity. This is shown in Figure 9 for the swelling in water of the homologous series of NBRs. The degree of swelling increases in time even after 350 h, and a constant value has yet to be reached. This phenomenon was also observed by Nijhuis et al.[32] The swelling behavior in time in a solution of 3.5*M* silver nitrate could not be determined experimentally: after 1 or 2 days, the NBR films were completely swollen and could not be handled anymore without destroying them because they did not have any mechanical strength and were soft and sticky.

X-ray fluorescence and atomic absorption spectroscopy

To determine the amount of Ag^+ ions in the permeate of pervaporation, and in the PDMS and EPDM films used for pervaporation and swelling, the permeate was analyzed using atomic absorption spectroscopy (AAS) and the polymer films were analyzed using X-ray fluorescence (XRF).

The AAS results show that the amount of silver ions in the permeate was $3.7 \times 10^{-3} \pm 2.6 \times 10^{-3}$ mol/L for PDMS and $4.8 \times 10^{-4} \pm 3.3 \times 10^{-4}$ mol/L for EPDM. The high error value was mainly caused by the small amount of sample collected during pervaporation with PDMS or EPDM. The result shows that, as expected, only negligible amounts of silver ions can pass the films.

The amount of silver ions in the films used for these pervaporation experiments and for the swelling experiments is given in Table III. Before analyzing, the membranes were dried for 72 h in a nitrogen oven at 30°C. The amount of silver ions in the films was calculated in $\mu g/mm^2$ and the thickness of the films was not taken into account because the distribution of the silver ions through the films did not have to be uniform because of a concentration gradient during pervaporation and swelling and because of evaporation of the water during drying of the films. Based on the structure of the matrix material and the amount of silver present in the material, the penetration depth of the radiation was determined to be considerably higher than the actual film thickness. The samples

TABLE III
XRF Results for Dried PDMS and EPDM Films Used for Pervaporation and Swelling

Membrane	Experiment	Membrane thickness (mm)	Amount Ag^+ ($\times 10^{-5}$, $\mu g/mm^2$)
PDMS	Pervaporation	0.20	4.6 ± 1.1
	Swelling	0.21	3.3 ± 1.2
EPDM	Pervaporation	0.07	3.5 ± 1.3
	Swelling	0.08	2.5 ± 1.0

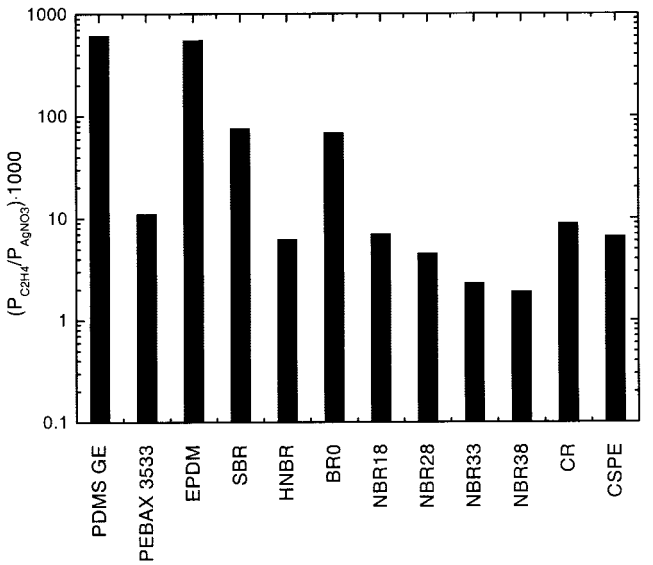

Figure 10 Ratio of ethylene permeability and water permeability (feed: 3.5*M* $AgNO_3$) for elastomers at $T = 25°C$.

were analyzed from both sides, the upper and the lower part of the film. In both cases, the same value was found, which can also be an indication that the complete sample is analyzed, and not only its top layer. The amount of silver ions in the films was low, indicating the low interaction of these polymers with silver ions. Because of the experimental error, no clear differences in the amount in PDMS or EPDM or differences between pervaporation and swelling could be distinguished.

SELECTION OF TOP LAYER MATERIALS

For selection of suitable top layer materials for application in gas–liquid membrane contactors for the separation of paraffins and olefins three parameters are of major importance:

1. The material should be highly permeable for olefins.
2. It should prevent pore flooding of the porous support.
3. It should have a low water permeability to avoid humidification of the feed stream.

A high permeability for the component to be removed (the olefin) and a low permeability for the absorption liquid (water from the silver nitrate solution) are particularly important criteria. The ratio of this gas and liquid permeability was therefore used as the selection criterion: generally speaking, the higher this ratio (relatively high ethylene permeability compared to relatively low water permeability), the more suitable the material for the current application. In Figure 10 this ratio of the ethylene permeability to the water permeability from an aqueous solution of silver nitrate (3.5*M*) is plotted for the elastomers investigated.

It is clear that PDMS and EPDM have the highest ethylene/water permeability ratio and are the most suitable materials for application in a gas–liquid membrane contactor for the separation of paraffins and olefins using a silver nitrate solution as absorption liquid. However, SBR, BR 0, and perhaps PEBAX 3533 and CR also fit the requirements fairly well. However, SBR and BR 0 are, because of the enormous swelling in a silver nitrate solution, mechanically unstable and therefore not appropriate candidates. PDMS and PEBAX 3533 have a relatively high water permeability, which could lead to humidification of the feed gases in a membrane contactor application. This high water permeability, however, is not visible in Figure 10 because of the compensating effect of the high ethylene permeability. The opposite is true for CR, which has a very low gas permeability; this is not clear from Figure 10 because of corresponding low water permeability.

Based on the screening experiments, ethylene propylene diene terpolymer (EPDM) is the most appropriate candidate with the highest potential for application in a gas–liquid membrane contactor for the separation of paraffins and olefins. It has a relatively high olefin permeability (46.4 Barrer) and a corresponding low water permeability and degree of swelling in a 3.5*M* silver nitrate solution (1490 Barrer and 0.14 wt %, respectively).

NOMENCLATURE

A	effective membrane area (cm^2)
c	concentration (m^3/m^3)
D_i	diffusion coefficient of component i (m^2/s)
E_a	enhancement factor attributed to chemical reaction (–)
E_p	activation energy for permeation (J/mol)
J	flux through the membrane ($m^3/m^{-2} \times s$)
K_{ov}	overall mass transfer coefficient (m/s)
k_g	mass transfer coefficient of the gas phase (m/s)
k_l	mass transfer coefficient of the liquid phase (m/s)
k_s	mass transfer coefficient of the porous support (m/s)
k_t	mass transfer coefficient of the dense top layer (m/s)
M	molecular weight (g/mol)
l	film thickness (cm)
m	distribution coefficient between top layer and liquid phase (–)
P_i	permeability of component i (1 Barrer $= 1.10^{-10}$ $cm^3 \times cm/cm^2 \times s \times cmHg$)
P_0	preexponential factor (cm^3 $cm/cm^{-2} \times s \times$ cmHg)

p_i	partial pressure of component i (cmHg)
S_i	solubility of component i in dense top layer ($cm^3/cm^3 \times cmHg$)
SD	degree of swelling (%)
R	universal gas constant ($J/mol \times K$)
T	temperature (K)
V_m	molar gas volume at STP (cm^3/mol)
$w_{swollen}$	weight of the swollen polymer (g)
w_{dry}	weight of the dry polymer (g)

This research was financially supported by the Centre for Separation Technology, a cooperation between the University of Twente, The Netherlands, and TNO, the Netherlands Organisation for Applied Scientific Research.

Louise Oude Vrielink from the Catalytic Processes and Materials group of the University of Twente and Annemarie Montanaro from the Chemical Analysis group of the University of Twente are highly acknowledged for performing the XRF and AAS measurements.

References

1. Gabelman, A.; Hwang, S.-T. J Membr Sci 1999, 159, 61.
2. Eldridge, R. B. Ind Eng Res 1993, 32, 2208.
3. Brandt, P. Acta Chem Scand 1959, 13, 1693.
4. Bessarabov, D. G.; Sanderson, R. D.; Jacobs, E. P.; Beckman, I. N. Ind Eng Res 1995, 34, 1769.
5. Westerterp, K. R.; van Swaaij, W. P. M. Chemical Reactor Design and Operation, 2nd ed.; Wiley: Chichester, 1987.
6. Kreulen, H.; Smolders, C. A.; Versteeg, G. F.; van Swaaij, W. P. M. Chem Eng Sci 1993, 48, 2093.
7. Cussler, E. L. In: Membrane Processes in Separation and Purification; Crespo, J. G.; Böddeker, K. W. Eds.; Kluwer Academic: Dordrecht, The Netherlands, 1994; p. 375.
8. Reed, B. W.; Semmens, M. J.; Cussler, E. L. In: Membrane Separation Technology, Principles and Applications; Noble, R. D.; Stern, S. A. Eds.; Elsevier: Amsterdam, 1995; p. 467.
9. Qi, Z.; Cussler, E. L. J Membr Sci 1985, 23, 321.
10. Qi, Z.; Cussler, E. L. J Membr Sci 1985, 23, 333.
11. Nijhuis, H. H.; Mulder, M. H. V.; Smolders, C. A. J Appl Polym Sci 1993, 47, 2227.
12. Mark, J. E. Polymer Data Handbook; Oxford University Press: New York, 1999.
13. Brandrup, J.; Immergut, E. H.; Grulke, E. A. Polymer Handbook, 4th ed.; Wiley: New York, 1999.
14. van Krevelen, D. W. Properties of Polymers, Their Correlation with Chemical Structure; Their Numerical Estimation and Prediction from Additive Group Contributions, 3rd ed.; Elsevier: Amsterdam, 1990.
15. Bondi, A. Physical Properties of Molecular Crystals, Liquids, and Glasses; Wiley: New York, 1968.
16. Nijhuis, H. H. Ph.D. Thesis, University of Twente, Enschede, The Netherlands, 1990.
17. Bos, A.; Pünt, I. G. M.; Wessling, M.; Strathmann, H. Sep Purif Technol 1998, 14, 27.
18. Meuleman, E. E. B.; Willemsen, J. H. A.; Mulder, M. H. V.; Strathmann, H. J Membr Sci 2001, 188, 235.
19. Bos, M.; Vrielink, J. A. M. Anal Chim Acta 1998, 373, 291.
20. van der Vegt, A. K. Polymeren, van Keten tot Kunststof; Delftse Uitgevers Maatschappij: Delft, 1994.
21. Kim, J. H.; Ha, S. Y.; Lee, Y. M. J Membr Sci 2001, 190, 179.
22. van Amerongen, G. J. J Polym Sci 1950, 5, 307.
23. Blackley, D. C. Synthetic Rubbers: Their Chemistry and Technology; Applied Science Publishers: London, 1983.
24. Blume, I.; Smit, E.; Wessling, M.; Smolders, C. A. Makromol Chem Macromol Symp 1991, 45, 237.
25. Stern, S. A.; Shah, V. M.; Hardy, B. J. J Polym Sci Part B: Polym Phys 1987, 25, 1263.
26. Daubert, T. E.; et al. Physical and Thermodynamic Properties of Pure Chemicals, Evaluated Process Design Data; American Institute of Chemical Engineers/Hemisphere: New York, 1989.
27. Freeman, B. D.; Pinnau, I. Trends Polym Sci 1997, 5, 167.
28. Merkel, T. C.; Bondar, V. I.; Nagai, K.; Freeman, B. D.; Pinnau, I. J Polym Sci Part B: Polym Phys 2000, 38, 415.
29. Merkel, T. C.; Bondar, V. I.; Nagai, K.; Freeman, B. D. Macromolecules 1999, 32, 370.
30. Winstein, S.; Lucas, H. J. J Am Chem Soc 1938, 60, 836.
31. Beverwijk, C. D. M.; van der Kerk, G. J. M. Organometal Chem Rev A 1970, 5, 215.
32. Nijhuis, H. H. Ph.D. Thesis, University of Twente, Enschede, The Netherlands, 1990.